Using JFOLD and LS-DYNA to Study the Effects of Passenger Airbag Folding on Occupant Injury

Richard Taylor[1], Shinya Hayashi[2], Mayumi Murase[2]

[1]Arup
[2]JSOL Corporation

1   Abstract

JFOLD is a software tool for simulation-based airbag folding in LS-DYNA®. This paper presents how JFOLD and LS-DYNA can be used effectively to research how slight changes in automotive passenger airbag folding can lead to significant changes in occupant injury prediction.

The demands placed on today's occupant safety teams continue to increase, driving up the need for airbag complexity and simulation accuracy whist driving down the time to deliver. Accurate airbag simulation is critical to improve occupant safety in an increasing number of crash scenarios and out-of-position cases, including passengers of autonomous vehicles. In addition, airbag simulation is now being used to assess the performance of interior trim components during early break-out and deployment.

However, accurately simulating the deployment of frontal passenger airbags (PABs) is still a challenging task for many involved in automotive safety. Not only is it hard to replicate the flattened 3D shape and hard to simulate the complex gas dynamics during deployment, but there is also a degree of natural variation in the fold pattern of real airbags due to manual folding processes which can lead to a variation in deployment behaviour and occupant injury. In addition, even well-made computer models of PABs can demonstrate sensitivities to initial conditions due to the high complexity of simulating gas flow though folded fabric.

As part of ongoing airbag simulation research at JSOL Corporation in Japan we present some recent work into the detailed modelling, folding and deployment simulation of a production passenger airbag, to share our solutions to some of the above challenges. We demonstrate how JFOLD's flow-chart folding process can quickly generate several variations of fold pattern and investigate the effect on occupant injury in commonly used loadcases. The latest features of JFOLD and airbag simulation in LS-DYNA will also be discussed.

2   Introduction

Slight variation in airbag folding is considered to be one of the contributing factors to deployment repeatability issues in passenger airbag design [1][2]. The folding process is often cited as a bottleneck when using simulation as a tool for airbag development and validation [2][3]. This study uses the new version of JFOLD to quickly generate four passenger airbag models with slightly different fold patterns, then compares predicted injury in two out-of-position loadcases using the Hybrid 3 6-year-old dummy.

2.1   Objectives of this study:

1.   Demonstrate JFOLD as an effective tool in the study of airbag folding variability
2.   Investigate effects of folding on injury in a challenging loadcase using CPM and LS-DYNA
3.   Document what we learned and share with others to help advance improvements in vehicle safety

When making an airbag model it is often difficult to judge whether the hem parts should be meshed and included, or represented simply by increasing thickness of nearby parts. In this study two baseline models were generated; one with all fabric hems attached and connected realistically, and one without outer hems, which is the more common approach.

2.2   Introducing JFOLD

JFOLD is a software tool developed by JSOL Corporation that helps the user perform simulation-based airbag folding. It runs inside Oasys PRIMER as a JavaScript and uses LS-DYNA® to simulate each folding step. The JFOLD graphical interface is designed to be easy to use and intuitive, so only a basic knowledge of LS-DYNA or PRIMER is needed. More information can be found in [4].
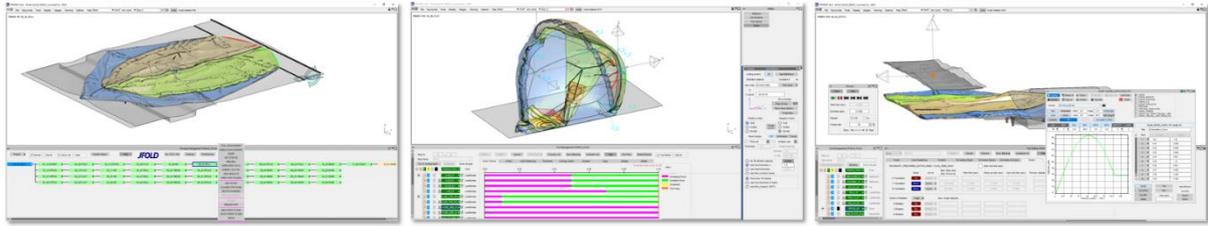
Fig.1:   *JFOLD's GUI: process management, tool management & tool setting panels*

JFOLD's special benefits
- Folding steps managed using flow-chart graphics
- One-click auto-positioning of tools, reusability of tools, fast user-defined tool generation
- Auto defined material properties and contact settings for folding
- Non-encrypted input files. Free, state-of-the-art example models to use as templates
- Airbag morphing function
- Direct LS-DYNA job submission. Error-free LS-DYNA initialisation
- A *Replace Airbag* function to quickly copy whole folding paths
- Checking for contact penetrations and over-stretched fabric

3   PAB Model

Several identical passenger airbags were purchased for this study. This airbag can be found in a popular small-sized passenger vehicle in Japan.

3.1   Geometry

CAD geometry was generated by scanning the fabric parts as shown in figure 2. This airbag can be laid flat in a semi-assembled condition; two panel edges can be sewn before the bag takes a 3D shape. The tether and inner airbag (more of a loop) can also be attached in a flat, pre-folded state.

Fig.2:   *Left: main panel semi-assembled, hem tucked inside, foldlines marked in pen. Right: tether, inner & wrapper.*

3.2   Assembly

The geometry was meshed using 2.5mm shells, in the semi-assembled condition shown in figure 3, to make folding easier. The tether was cut in two, with the wide panel upright and hole end laid flat and pre-stitched to the rest of the bag. This helped establish the correct tether location in the first fold step.
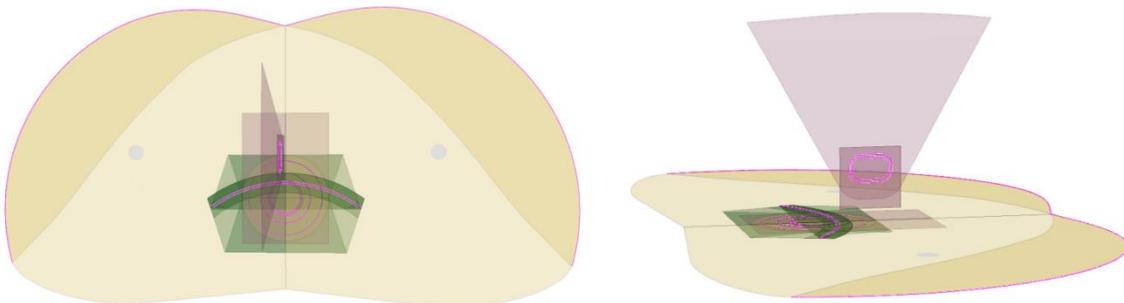

Fig.3:   *PAB model (no outer hems) in semi-assembled condition*

Seam lines were modelled using a single row of narrow shells as a wall that spans the airbag panels. This means fabric panels can be kept flat (easy to mesh), seam stiffness can be tuned in lateral and longitudinal directions and multiple layers of stitched fabric have the correct sectional properties. Occasional contact penetration at the seam can be mitigated by using SFNBR=1 (in R11.2.2).

In the model with no outer hem, the thickness of shells over a similar width around the perimeter was increased to represent the higher mass and stiffness. The inner airbag (shown in green above) has all seam reinforcement fabric included in all models. This was considered important for keeping the inner bag stable under high jetting pressures, to allow particles to be redirected sideways.

4 PAB Folding using JFOLD & LS-DYNA

Four folded models were generated for this study, shown in figure 4:
1. Baseline foldlines with all hem fabric included
2. Baseline foldlines without the outer hem parts (foldlines identical to 1)
3. Variant 1 (no hem) with foldlines rotated $+2^0$ to represent natural variation
4. Variant 2 (no hem) with foldlines rotated -2^0 to represent natural variation

Foldlines were created by importing a photograph to the background of a common meshing tool, lining up the fabric panels then generating CAD lines where the main foldlines are visible. Left and right sides were averaged. The lines then were meshed as chains of 2.5mm null beams, in-plane with the shells but independent of them. The beams were attached to the fabric using TIED NODES TO SURFACE OFFSET (penalty type, so beams can be used in other constraint conditions – modifiable within JFOLD). Two simple model variants were created by rotating the foldline beams approximately +/- 2^0 in two locations as shown on the right in figure 4. The foldline beams are ~30mm apart at the widest.
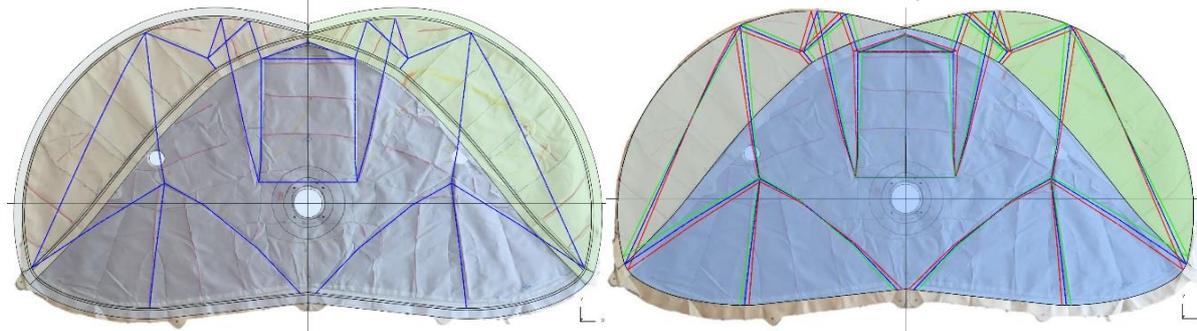

Fig.4: Left: PAB with hem, foldline beams in blue. Right: Simple no-hem model, three foldline patterns in red, green and blue superimposed

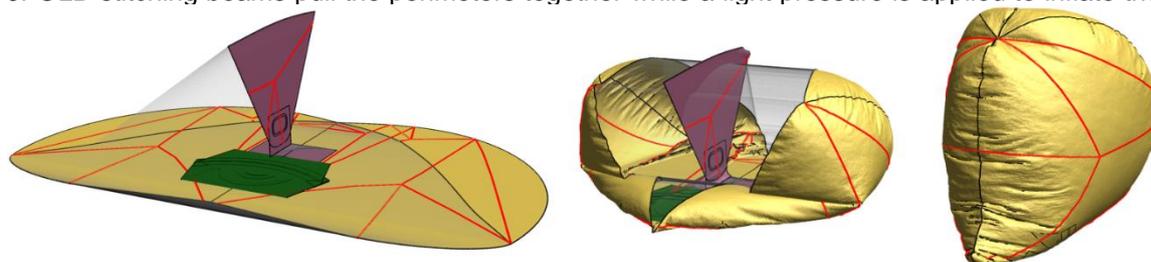### 4.1 Detailed model with hem

The first model with outer hem took on average two days to fold each step, as various folding methods were tested and assessed for quality and fidelity. Each step took between 20 minutes to 1 hour on 64cpu, (analysis time 50~100ms). The following images highlight some steps in more detail.

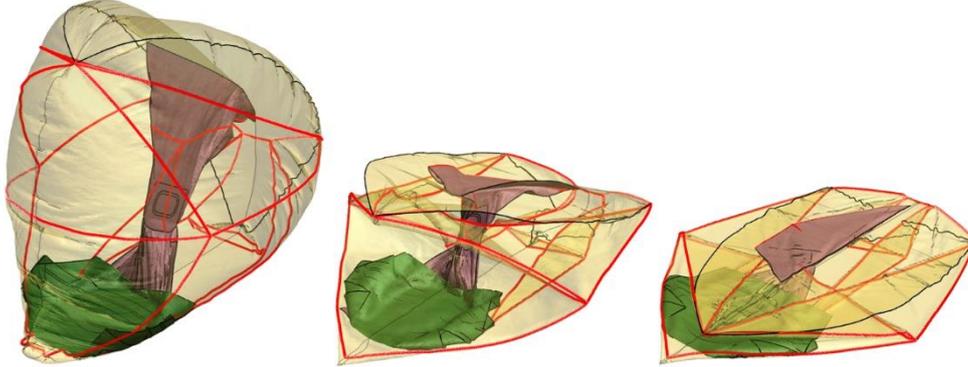Fig.5: The JFOLD project fold steps created for the baseline model with outer hem

4.1.1 Step 1: INFLATE & STITCH

JFOLD stitching beams pull the perimeters together while a light pressure is applied to inflate the bag.
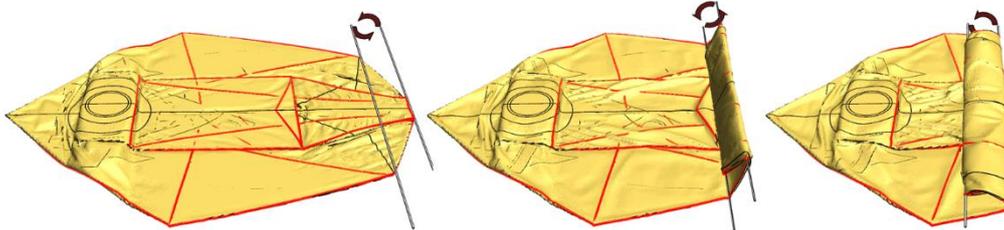
4.1.2 Step 2: FLAT

Load is applied to the foldline beams (shown in red) to collapse the bag into a 2D condition. The tether was collapsed at the same time using the same method. For more information on this method, see [4].
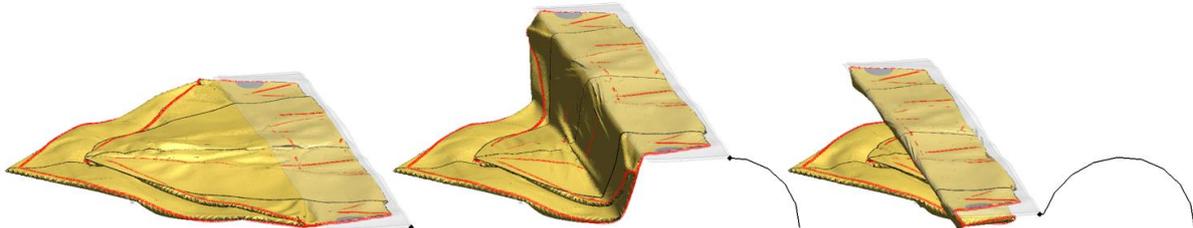

4.1.3 Step 4: ROLL

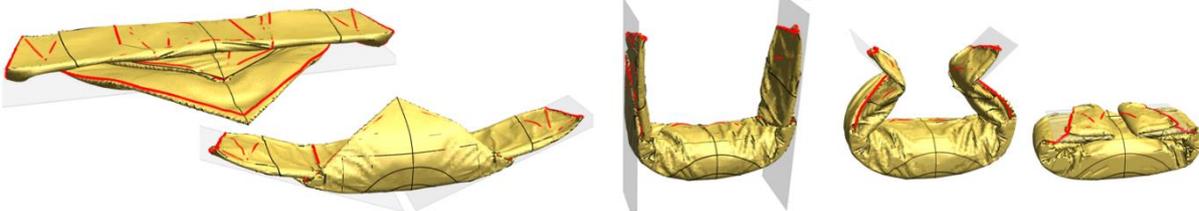Simple set-up using two rods and JFOLD's ROLL tool, making two full rotations.

4.1.4 Step 6: Z-FOLD

In a prior step, pressure was applied to a deformable plate to flatten the roll. The plate was then used in this step as a rigid Z-FOLD tool, to lift the roll up and over the top of the airbag.
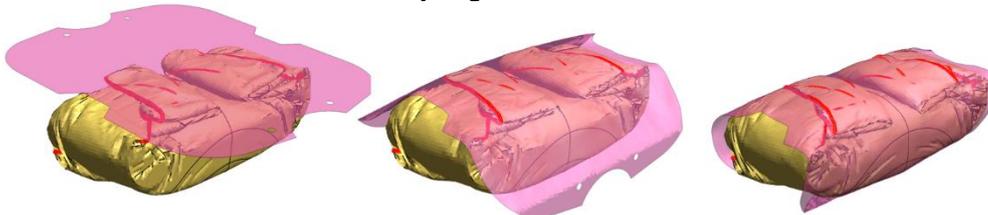

4.1.5 Steps 7 & 8: BEND then FOLD

The front corner was folded using load and pressure, then two tools rotated the sides vertical. In the next step the plates were scaled down and used to fold the remaining sides down to the centre.

4.1.6 Step 9: WRAP

The final step was to wrap the cover around the folded airbag. Tools with circular motion pulled the wrapper bolt holes around the sides until they aligned with the retainer bolts.

4.1.7 Extra Steps for With-Hem Model

The detailed model with outer hem required two additional steps at the beginning to invert the side panels, pushing the hem inside the bag. As shown in figure 6, first the side panels were pushed inside out using pressure and edge loads, then folded outwards using plates and pressure.
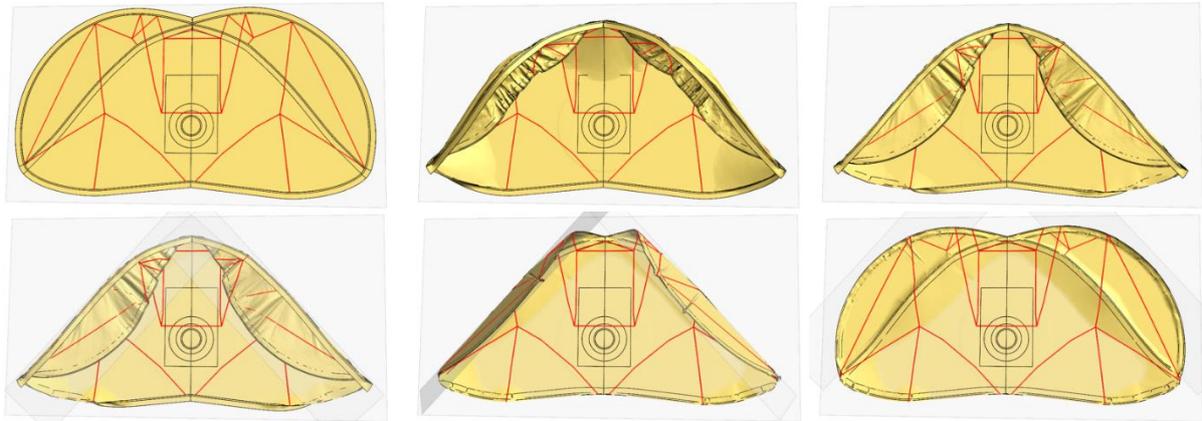

Fig.6: Turning the pre-stitched side panels inside out so that the hem lies on the inside

4.2 Fidelity of the Folded Model

The folding techniques were developed to ensure the model looks like the real airbag at every step.

Fig.7: Top and bottom views, after flattening & fitting retainer (with-hem model)

Fig.8: View from below during ROLL folding

Fig.9: After folding, before fitting wrapper

Care was taken during inflator fitting to ensure the correct location of the inner hem directly above the inflator (the green part in figure 10). These surfaces are the first to be pressurized by inflator gas/particles, so correct location & material stiffness in the model help achieve accurate initial deployment.

Fig.10: Folded & fitted with retainer & wrapper, view from below.

4.3 Copying fold paths and variant airbags

Once the first airbag was complete, COPY PATH was used to copy all steps for the next:

Fig.11: Copying all steps from the first airbag to fold a new one

The second airbag without the hem was treated by JFOLD as a completely new model: node and shell sets in some steps had to be re-created but otherwise all tools could be re-used with little/no modification. The AUTO MOVE function was used to quickly reposition tools where needed. The final two fold patterns were identical to the second except for node co-ords of the foldline beams, so REPLACE AIRBAG could be used (new in JFOLD ver. 8.0) where all node and shell sets were retained.
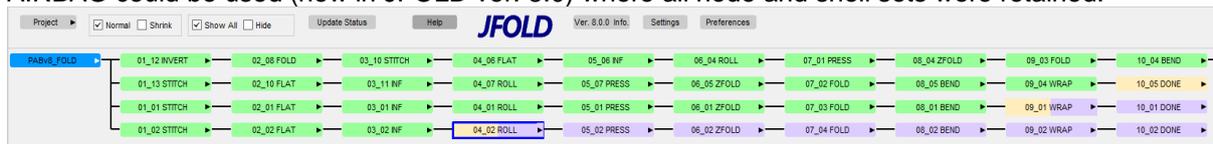

Fig.12: Running the final two variants concurrently

For these final two fold patterns several steps per day could be analysed, and different airbags run at the same time. In future JFOLD versions analysis submission will be more automated, including automatically applying the AUTO MOVE tool capability.

4.4 Comparison of Models, Mid-Fold

Figure 13 shows the four models after the flattening step. From left: Baseline with hem, Baseline no-hem, Variant 1 no-hem, Variant 2 no-hem. Very little difference in foldline location or folded shape can be seen at this stage. The level of variation is similar to that seen in the real airbags used in this study.
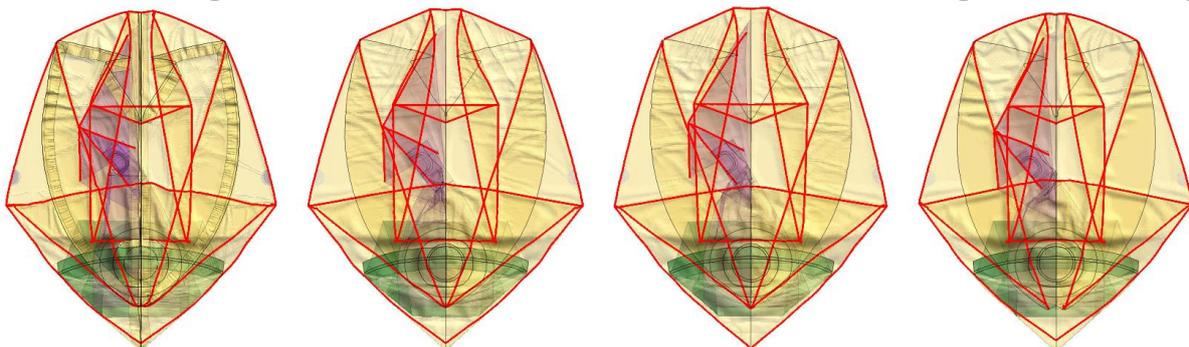

Fig.13: The four PAB models used in this study, mid-fold.

4.5 Checking and assessing the fold after each step

JFOLD reports contact penetration and mesh distortion. Penetrations and crossed edges can be investigated and fixed using PRIMER's pencheck tool. The distorted mesh check plots magnitude Green-Lagrange strain (calculated using reference geometry and local material axes like LS-DYNA). A percentage of shells above a certain threshold strain can be visualized to get a quick overview of the level of residual stretch caused by the previous step. Experience suggests strains above 0.1 should be avoided, but this depends on the application. In the example below, 7% of elements are reported to

have 0.01 or higher strain, which is a very good result. 7 crossed edges are reported which were quickly fixed by hand from within JFOLD using PRIMER's pencheck fixer. Anything up to 20~30 crossed edges can be fixed in under 10min by an experienced user.
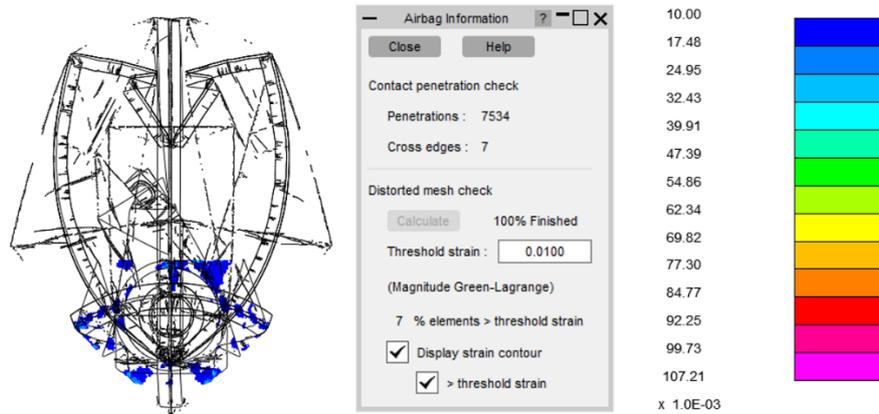

Fig.14: JFOLD's quality checks include number of crossed edges and residual strain

5   Inflator Characterization & Static Deployment

5.1   Tank Test Analysis

Inflator data available at the time of this research was limited to:
- Total mass, from weighing inflators pre- and post-fire
- 60 litre tank test pressure curves (2 repeats)
- Gas composition (mole fractions, from supplier)

From this, inflator mass-flow & temperature curves were estimated using a technique that bases the mass-flow curve on the differential of the tank pressure curve (as described in [5]). A CPM model of the tank, including mixing with initial air and heat loss (HCONV 0.2mW/mm^2.K) to the tank wall was used to refine the inflator temperature input until pressure matched test. Far better methods are used by suppliers to generate more accurate inflator data, but for the purposes of this study this approach was acceptable. A total of 95,000 particles were used (4x this only changed the pressure result by 0.2%).

A ratio of 0.9 for air:gas (NPAIR=45,000, NP=50,000) resulted in the closest matching curves for the four methods of pressure measurement in LS-DYNA. These are:
1.   "Airbag pressure, P (IE)", summing partial pressures, T from IE & C_P, assumes thermal equilibrium
2.   "Particle pressure, P (KE)", from kinetic energy of all particles & tank volume
3.   "Part pressure", from summed particle impact momentum, smoothed over time
4.   "CPM SENSOR pressure", from KE of particles in sensor, weighted towards the centre

Ratios from 0.8 to 1.22 were studied by varying NPAIR. P(KE), part and sensor pressures are all related to particle velocity and reported similar pressures every run but depending on the ratio they were all slightly different to P(IE), which changed little regardless of ratio. The 1.22 ratio recommended by LS-DYNA (based on matching mole/particle), resulted in a ~1.5% difference between P(IE) and the other methods. Although not much, this could compound with other inaccuracies to cause trouble when trying to correlate later. A general formula for ideal ratio (other than mole/particle) is worth further investigation.
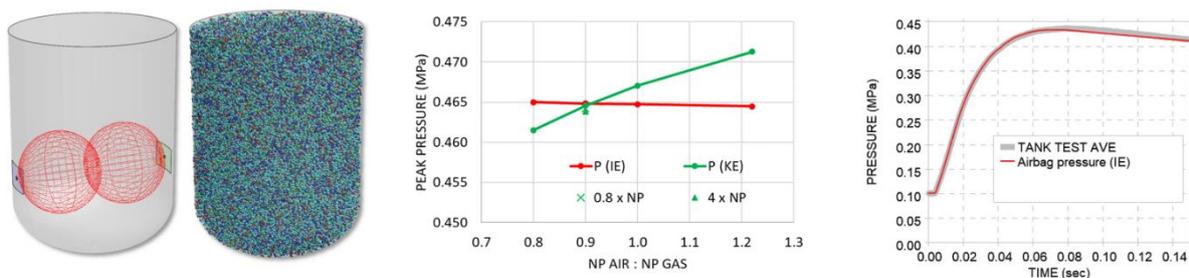

Fig.15: Left: tank test model with CPM sensors. Middle: differences in peak pressure reported by "Airbag pressure" P (IE), and "Particle pressure" P (KE) for varying ratios of NP air:gas. Right: tank test vs. analysis pressure P(IE)

5.2 Static Deployment Correlation

Simple static deployment tests were performed to correlate the early stages of inflation in a controlled environment. Tests to record pressure and a dynamic impactor were not included but are planned for future work. The baseline models were set up as test and deployed using CPM inflator data from the tank test analyses shown previously. Results are shown in figures 16 and 17.

The following modelling parameters were found to influence early stages of deployment:
1. Jet orifice arrangement, initial air particle placement, material compressive stiffness, inflator curves
2. Inner airbag stiffness, inner hem model, particle redirection using VANG=-2

Fig.16: Static deployment vs test, view from side (2ms between frames)
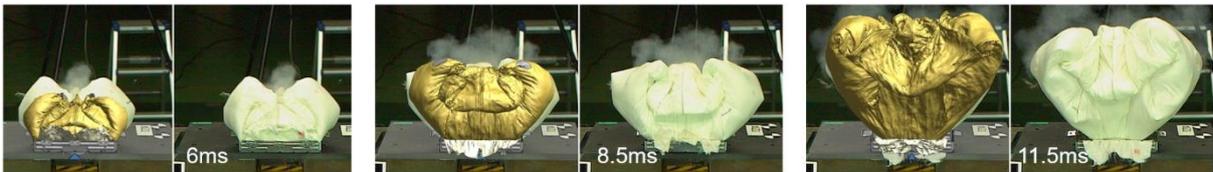

Fig.17: Static deployment vs. test, from rear

Good agreement to test deployment shape was achieved by ensuring a realistic (stiff) inner fabric structure with realistic orifice jet locations and angles to open up gaps. A limited number of orifices were used with vectors and cone angles to represent the real gas flow redirection by the retainer (see [6]). A small amount of low compressive stiffness was used in the outer fabric to encourage gap opening.

Inner vents were made using zero-stiffness null shells spanning the inner bag exit holes left and right. The VANG=-2 setting was used which controls particle direction after passing through the inner vents. A 45^0 angle was found to give the best result, gradually rotating to the horizontal. A loadcurve LCRED was used to limit this function to just the early deployment phase. (See [5] for more details.)

The left image in figure 18 shows the initial jet pressure on the inner structure and gaps opening up. The middle & right images contour particle flow velocity after passing through the vents at 45^0.
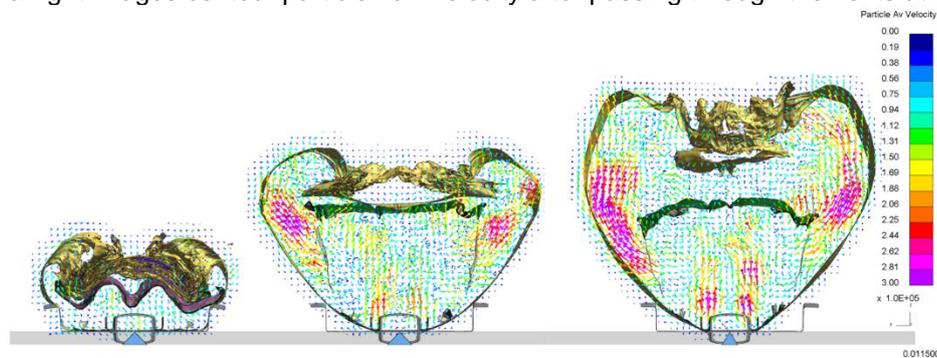

Fig.18: Averaged/smoothed particle flow velocity at 6ms, 8.5ms & 11.5ms, visualized in Oasys D3PLOT

6   OOP Sled

6.1   Sled model

The sled model was based on the 2012 Toyota Camry model developed by Center for Collision Safety and Analysis [7]. The vehicle was cut down to just the front passenger side occupant compartment, the instrument panel (IP) cut along the vehicle center line and nodally constrained. Body panels were made rigid for efficient run time, their presence only required for contact, connection or visual reference. The Camry simplified PAB, chute and attachment brackets were replaced with detailed models created for this research.

The new metal case geometry was based on 3D scan data. A new plastic chute model with hinged lid attached to the IP a-surface was created and meshed to fit the Camry geometry. Although this chute does not exist in real life, great care was taken to ensure that the geometry, materials (with failure) and functionality closely resembled real chute and lid designs modelled in previous consulting projects. To observe the effect that the lid may have on airbag deployment and dummy injury, each loadcase was analysed with and without the chute lid.
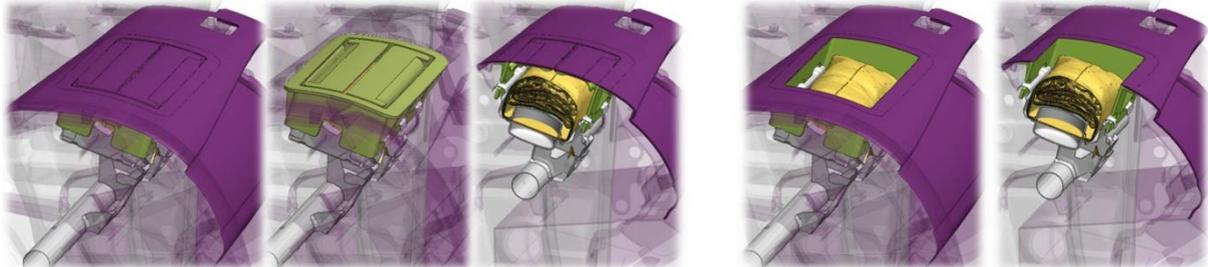

Fig.19:   Left: IP & chute with lid.   Right: chute without lid.

6.2   Deployment Without Occupant

The four airbag models were deployed in the sled condition without occupants to check contacts, fabric distortion and measure airbag energies in a relatively load-free condition. It was found that airbag volume varied by less than 2%. Models with lids recorded peak break-out gauge pressures around 15% higher than those without, but at the time of occupant impact gauge pressure for all cases varied by around 8%.

In Figure 20 the left graph shows airbag energies for all four airbag models with and without chute lids: eight cases in total. Dashed lines are used for the cases with no lid. Differences are barely visible.
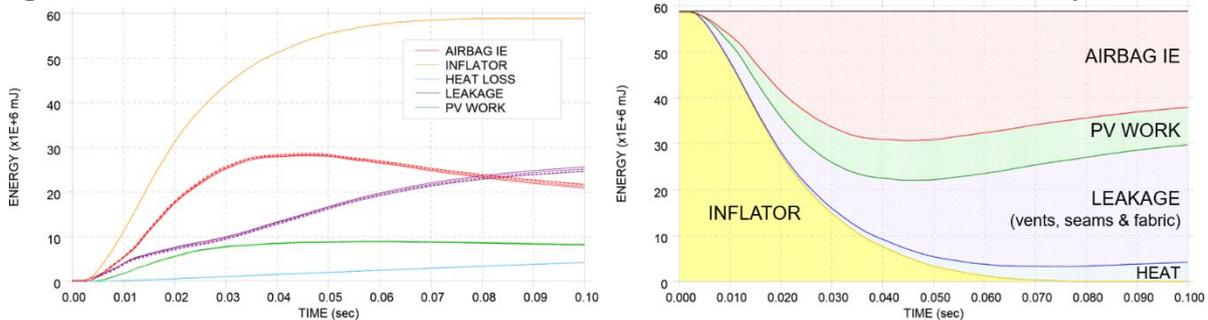

Fig.20: Airbag energies without dummy. Left: all cases, right: energy flow in a typical case

LS-DYNA outputs energies for airbag internal, inflator, leakage and heat loss. Ignoring initial air, contact and damping energy, the "PV-work" in each case can be calculated. This is the work done to inflate the airbag and push against its surroundings. Only a tiny difference in PV-work is noticeable from 4ms, suggesting the lid has little effect on the energy remaining in the airbag.

The graph on the right is an alternative way of visualizing the energy transformation during deployment. The inflator energy curve has been inverted so at 0.0ms, 60kJ starts inside the inflator. As the gas particles are released the 60kJ is converted to one of the four energies on the right. Leakage energy could be separated into vents, seams and fabric porosity, which can be useful when designing vent hole size. (It was lumped together here for simplicity).

6.3 Low-Risk Deployment Loadcase Set-Up

The 6-year-old dummy out-of-position (OOP) loadcases described as NHTSA Positions 1 and 2 in FMVSS208 [8] were chosen for this study as they provide a sensitive mechanism to assess airbag deployment variation.
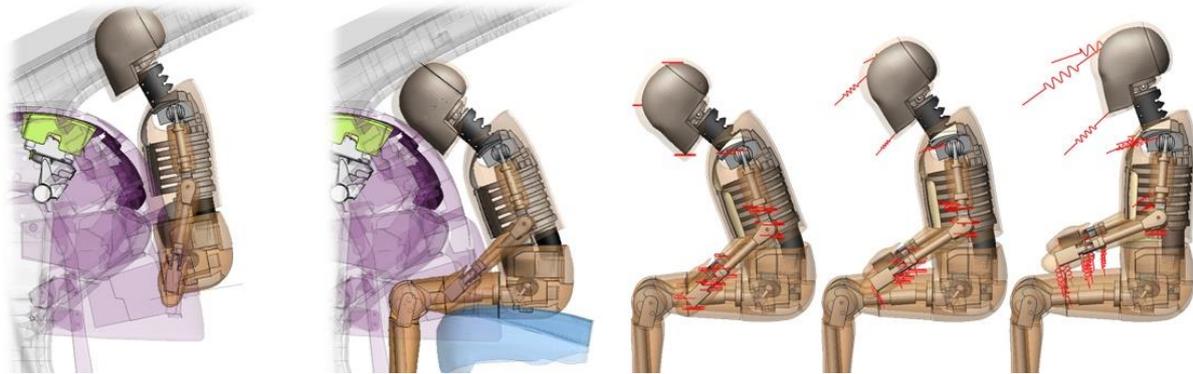

Fig.21: OOP loadcases, left: Position 1, middle: Position 2, right: positioning using PRIMER & LS-DYNA

This study used the free Hybrid-3 6-yr-old dummy model jointly developed by LST and the National Crash Analysis Center (NCAC) [9]. Modifications were made to improve results and enhance positioning. It was not possible to determine the exact dummy positions according to FMVSS208 due to lack of detail in the Camry seat model, so they were estimated based on other seats and published OOP studies.

Setting up the dummy for Position 2 can be time consuming as it requires pushing on the dummy back to deform the spine until the head touches the IP (as described in [1]). A PRIMER positioning tree file was created with extra joints at the top and bottom of the spine and base of the neck. The dummy torso could then be rotated fully forward during the PRIMER set-up phase, then the spine and neck rubber actually bent as the dummy is pulled into position by LS-DYNA. From PRIMER 18.0, LS-DYNA pre-simulation can be submitted direct from the software, but the whole task still requires care & effort.

A simplified seat model was made for Position 2 using a type 4 RIGID BODY ONE WAY TO RIGID BODY contact between the dummy and rigid seat cushion outer shells. An appropriate force-deflection curve was input to represent compression in the real cushion. Although considered good enough for this study, an accurate seat model is highly recommended for actual low-risk deployment assessment.

Friction values used were based on experience: Dummy to PAB: μ=0.3, PAB self-contact: μ=0.1, all other contacts: μ=0.2. Experience shows that injury may be highly sensitive to small changes in friction, but studies of this were not included in this phase of research.

6.4 OOP Results

Injuries were post-processed according to FMVSS208 test procedure using FAST-TCF, a scripting language for Oasys T/HIS which includes built-in post processing tools like filtering, head injury criterion (HIC) and normalized neck injury criteria (NIJ) [10]. Critical Values used for NIJ: 2800N tension, 2800N compression, 93Nm flexion, 37Nm extension, e=17.3mm (distance from loadcell to condyle joint).

Graphs of neck injury are shown below. On each graph there are eight curves for four airbag fold patterns, with and without chute lid. Models without lid are shown by curves in a lighter shade. Black dots indicate max or min values. Horizontal thresholds represent the maximum allowable injury values; curves falling within the red zones fail the assessment. Peak values of all assessed injuries are shown in the tables below. Each model took around 3.5 hours to 100ms on 64cpu (single precision R11.2.2).
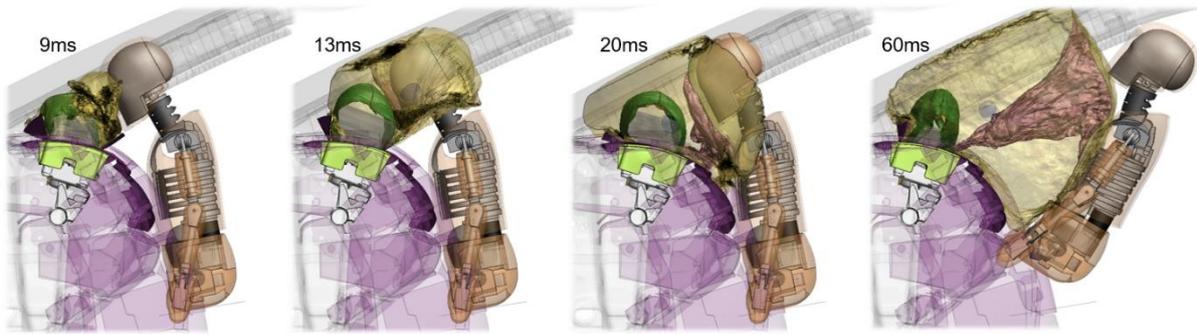
6.4.1 Position 1

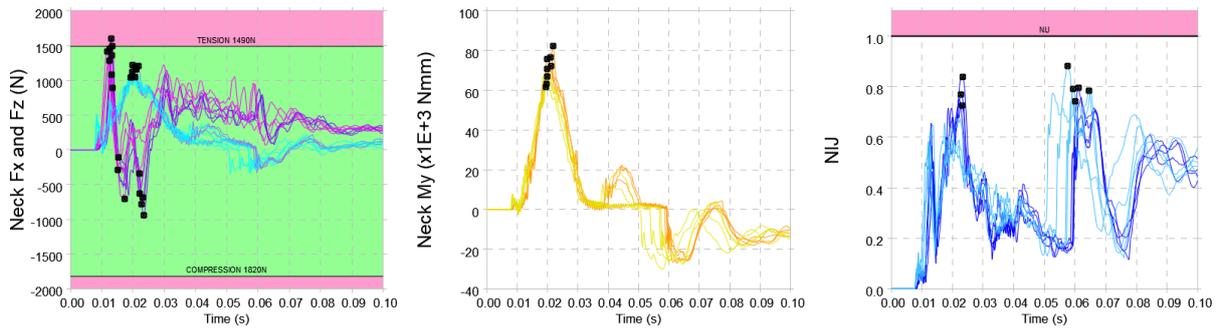

Fig.22: Key events during Position 1 deployment

Fig.23: Neck injury for 6-year-old in OOP NHTSA Position 1

Position 1	Outer	Chute	HIC		NIJ		Neck Tension		Neck Compression		Chest g		Chest Compression	
Foldline pattern	hem	lid	(-)	max	(-)	max	(N)	max	(N)	max	(g)	max	(mm)	max
Baseline	yes	yes	189	700	0.73	1.0	1082	1490	685	1820	48	60	17	40
Baseline	no	yes	187	700	0.84	1.0	892	1490	941	1820	46	60	16	40
Variant 1	no	yes	207	700	0.80	1.0	1601	1490	629	1820	46	60	15	40
Variant 2	no	yes	178	700	0.77	1.0	1361	1490	782	1820	43	60	15	40
Baseline	yes	no	178	700	0.88	1.0	1283	1490	289	1820	41	60	16	40
Baseline	no	no	163	700	0.78	1.0	1455	1490	341	1820	37	60	17	40
Variant 1	no	no	171	700	0.74	1.0	1416	1490	108	1820	41	60	15	40
Variant 2	no	no	185	700	0.79	1.0	1493	1490	706	1820	43	60	15	40

Table 1: Injury assessment for 6-year-old in OOP NHTSA Position 1

Neck tension at 13ms, when the airbag deploys up into the face, varied from 892N (pass) to 1601N (fail). The only model difference between these two extreme cases was a foldline rotation of 2^0. The baseline *with* outer hem was more severe than *without* outer hem when the lid was present, but less severe when it was not. In general, models without lid predicted slightly lower My & Fz peaks in flexion at 20ms but similar/slightly higher peaks in extension at 60ms. The chute lid did not hit the face when opening.
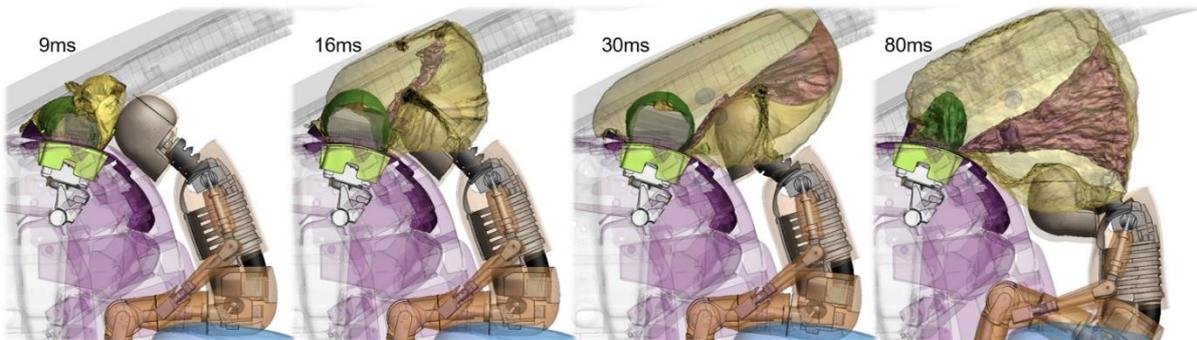
6.4.2 Position 2

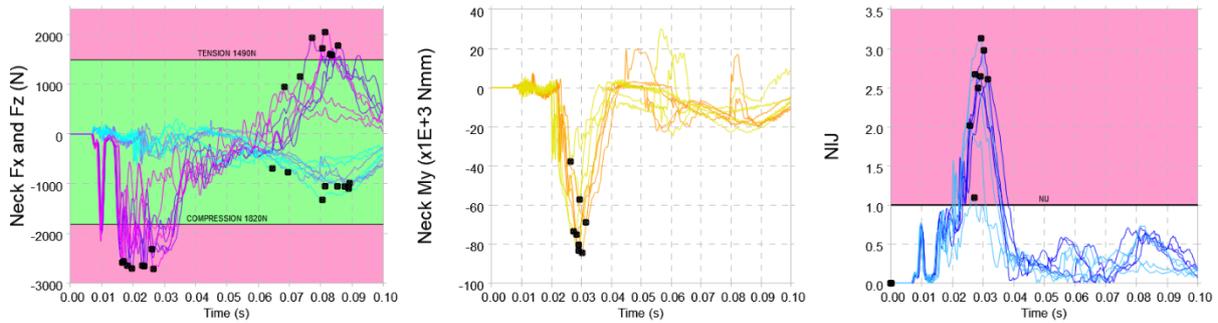*Fig.24: Key events during Position 2 deployment*

Fig.25: Neck injury for 6-year-old in OOP NHTSA Position 2

Position 2	Outer	Chute	HIC		NIJ		Neck Tension		Neck Compression		Chest g		Chest Compression	
Foldline pattern	hem	lid	(-)	max	(-)	max	(N)	max	(N)	max	(g)	max	(mm)	max
Baseline	yes	yes	99	700	2.5	1.0	1601	1490	2647	1820	28	60	5	40
Baseline	no	yes	153	700	3.0	1.0	1930	1490	2657	1820	28	60	6	40
Variant 1	no	yes	128	700	2.6	1.0	1584	1490	2646	1820	25	60	6	40
Variant 2	no	yes	146	700	2.6	1.0	1775	1490	2704	1820	30	60	7	40
Baseline	yes	no	107	700	2.7	1.0	1718	1490	2316	1820	25	60	3	40
Baseline	no	no	112	700	2.0	1.0	1151	1490	2585	1820	34	60	4	40
Variant 1	no	no	96	700	1.1	1.0	944	1490	2558	1820	32	60	5	40
Variant 2	no	no	136	700	3.1	1.0	2045	1490	2713	1820	26	60	6	40

Table 2: Injury assessment for 6-year-old in OOP NHTSA Position 2

Neck injury in Position 2 was much more severe than Position 1, with all cases failing NIJ. There was also greater variation in the magnitude of My and timing of Fz peaks. First peaks in neck compression at 10ms were very similar (the lid hit the head, but this made little difference) but diverged from 15 to 30ms.

The cause of this appears to be the behaviour of the roll: at first it is forced up through the narrow gap between the inner airbag and lid/head, then as the bag inflates the roll is slowly dragged over the surface of the head, as seen in figure 26. The four airbags may have very similar fold pattern but tiny differences in fold location in the mesh become amplified by this complex kinematic interaction between roll of fabric and dummy skin. Reducing contact friction (currently 0.3) may reduce variation. Null shells were added to span the gap between front and rear head skin, to avoid fabric getting caught.
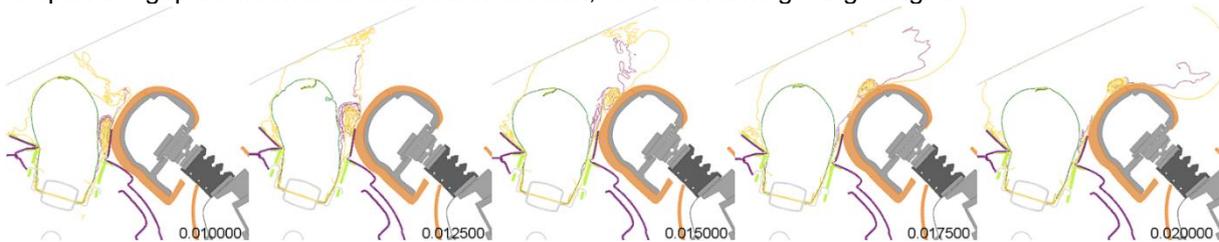

Fig.26: Cut section showing movement of roll over dummy head (with-lid case)

6.5   OOP Results Discussion

The results show that these loadcases were very sensitive to small differences in airbag fold pattern, hem model and module lid. However, the contribution that foldline differences had to variation in injury is difficult to assess without further study. An approach as described in [11] that uses a software tool such as DIFFCRASH may provide valuable insight.

Another logical next step would be to extend the study to real airbags and out-of-position tests. Access to physical test data throughout this research was limited. For real work on airbags, thorough multi-level validation to physical testing (as described in [12]) is highly recommend. It should also be noted that the airbag used in this study may not have been designed for 6-year-old OOP loadcases, and the model may be overpowered. Design changes such as using two side tethers, a v-shape volume or different roll pattern may all reduce injury and sensitivity to small changes in input.

The question of whether the outer hem is required for accurate simulation cannot be answered with without real airbag testing. The hem had no effect on static deployment kinematics. In the sled, the with-hem model predicted higher neck tension in Position 1, but the mechanism was not confirmed due to lack of time. Including the hem in the folding process took considerable more time and effort, so until more research is conclusive, no-hem would still be the recommended approach. (Adjustments to local shells should be made to account for missing hem mass and stiffness.) For the inner airbag, modelling all hem, seams and reinforcements is highly recommended.

Although now widely used in industry, the corpuscular particle method is physically limited in its ability to simulate gas flow through airbags, providing more of a moving pressure front with coarse pressure distribution behind. For simple airbags this is sufficient. For more complex airbags, CPM can sometimes be manipulated to achieve reasonable deployment behaviour (as seen in figures 16 & 17), however this requires careful judgement, understanding and produces bespoke solutions for each airbag. The PAB in this study benefitted from select orifice modelling and inner vents with VANG to influence particle flow. (Many other tuning parameters are available to stretch the capabilities of CPM).

For airbag simulation to be included in virtual vehicle development, wider access to accurate material data, more expertly derived inflator input and a more work on fluid solvers for airbag gas mechanics is required.

7 Summary

In this research JFOLD was used to fold a production-level passenger airbag quickly and accurately, using the foldline beam technique. Variations in foldline location were generated and quickly re-folded using JFOLD's new REPLACE AIRBAG function.

A realistic sled model was created and two out-of-position loadcases analysed using the 6-year-old dummy. A high degree of variation was observed in neck injury, due to the complex interaction between deploying airbag roll and dummy. Sources of this variation and its mitigation were discussed.

Various modelling techniques and settings for CPM were presented. Internal research findings, tips and new information are continuously added to a CPM Training Course for further knowledge dissemination [5].

Future JFOLD developments are focusing on increasing automation, tool functionality and user experience. World-wide customer feedback and requests drive continual improvement.

Research into airbag deployment in LS-DYNA continues with support for LST's development of a new fluid solver, customer training and support for JFOLD and CPM, towards the shared goal of virtual vehicle development.

8 Literature

[1] Feng, B.: "Low Risk Deployment Passenger Airbag – CAE Applications & Strategy", 14th International LS-DYNA Users Conference, 2016

[2] Feng, B.: "Challenge of Airbag Simulation for Airbag Deployment", Automotive CAE Grand Challenge 2015

[3] Christ, A., Büttner, J.: "Detailed Passenger Airbag Modelling for Early Stage Events", 2012 LS-DYNA Forum, Ulm

[4] Taylor, R., Hayashi, S.: "Airbag Folding with JFOLD – Latest Developments and Case Studies", 11th European LS-DYNA Conference 2017, Salzburg, Austria. See also https://www.jsol-cae.com/en/product/structure/jfold

[5] Taylor, R.: "Airbag Particle in LS-DYNA, v5.2", Arup CPM Training Course, 2021

[6]   Ida, H., Aoki, M., Asaoka, M.: "A Study Of Gas Flow Behavior In Airbag Deployment Simulation", 24th Enhanced Safety of Vehicles Conference, Gothenburg, Sweden, 2015

[7]   Marzougui, D., Brown, D., Park, C.K., Kan, C.D., Opiela, K.S.: "Development & Validation of a Finite Element Model for a Mid - Sized Passenger Sedan," 13th International LS-DYNA Users Conference, 2014. https://www.ccsa.gmu.edu/models/2012-toyota-camry/

[8]   U.S. Department Of Transportation, National Highway Traffic Safety Administration: "Laboratory Test Procedure For FMVSS 208, Occupant Crash Protection TP208-14", April 16, 2008

[9]   https://www.lstc.com/products/models/dummies/H3_6yo

[10]   Oasys T/HIS 18.0 manual, Appendix E.
        https://www.oasys-software.com/dyna/wp-content/uploads/2021/04/THIS-manual-18.0.pdf

[11]   Brown, R., Bloomfield, M., Thole, C-A., Nikitina., L.: "Analysis of the Scatter of a Deploying Airbag", 12th International LS-DYNA® Users Conference, Detroit, 2012

[12]   Lin, C.H., Cheng, Y.P.: "Evaluation of LS-DYNA CPM – Passenger Airbag Applications", 15th International LS-DYNA Users Conference, 2018